

2003

Ferroelectric-field-induced tuning of magnetism in
the colossal magnetoresistive oxide
 $\text{La}_{1-x}\text{Sr}_x\text{MnO}_3$

X. Hong

A. Posadas

A. Lin

C. H. Ahn

Follow this and additional works at: <https://digitalcommons.unl.edu/physicshong>



Part of the [Atomic, Molecular and Optical Physics Commons](#), and the [Engineering Physics Commons](#)

Ferroelectric-field-induced tuning of magnetism in the colossal magnetoresistive oxide $\text{La}_{1-x}\text{Sr}_x\text{MnO}_3$

X. Hong, A. Posadas, A. Lin, and C. H. Ahn

Department of Applied Physics, Yale University, New Haven, Connecticut 06520-8284, USA

(Received 28 July 2003; published 8 October 2003)

A ferroelectric field effect approach is presented for modulating magnetism in the colossal magnetoresistive oxide $\text{La}_{1-x}\text{Sr}_x\text{MnO}_3$ (LSMO). The ferromagnetic Curie temperature of ultrathin LSMO films was shifted by 35 K reversibly using the polarization field of the ferroelectric oxide $\text{Pb}(\text{Zr}_x\text{Ti}_{1-x})\text{O}_3$ in a field effect structure. This shift was also observed in magnetoresistance measurements, with the maximum magnetoresistance ratio at 6 T increasing from 64% to 77%. This model system approach does not introduce substitutional disorder or structural distortion, demonstrating that regulating the carrier concentration alone changes the magnetic phase transition temperature and leads to colossal effects.

DOI: 10.1103/PhysRevB.68.134415

PACS number(s): 73.50.-h, 75.47.Gk

The diverse behavior exhibited by correlated oxides originates from competing interactions, such as strong Coulomb repulsion and electron-phonon coupling. In the colossal magnetoresistive (CMR) manganites, this competition leads to strong correlations between the structural, transport, and magnetic properties. The origin of these correlations, the role of charge carriers, and their interplay with spin and lattice degrees of freedom are central issues that are still under debate.¹⁻³ The complexity of this problem is further increased by the intrinsic inhomogeneity of these materials.

Recent theoretical progress has shown that substitutional disorder has a significant effect on the critical temperature.⁴ The correlation between the Curie temperature and the residual resistivity in these materials has been suggested as the signature of a disordered system.⁵ It has also been proposed by Dagotto and co-workers that competing ordered states, combined with quenched disorder, dominate the macroscopic colossal effects observed in the transition metal oxides.⁶ As a result, experiments with the ability to probe different ordered states of these materials using the carrier concentration as a parameter, independent of the complicating effects of substitutional disorder and structural distortion, are required to clarify the role of charge density in the CMR effect.

In this paper, we present an electrostatic field effect approach to modulate the magnetic transition temperature and magnetotransport properties of the colossal magnetoresistive oxide $\text{La}_{1-x}\text{Sr}_x\text{MnO}_3$ (LSMO) by reversibly injecting and removing charge carriers in a field effect structure. This approach does not introduce disorder into the system, demonstrating that at fixed disorder, modulating the carrier concentration alone can lead to colossal effects in correlated oxide systems.

Doped LaMnO_3 (LMO) is a prototypical CMR material, whose electronic properties depend sensitively on carrier concentration.⁷ At zero temperature, undoped LMO is a canted antiferromagnetic (AF) insulator. When doped with holes via Sr substitution, transitions to ferromagnetic insulating (FI) and ferromagnetic metallic (FM) behavior occur (Fig. 1). The CMR effect is most pronounced near the Curie temperature (T_C), where for doping levels x between 0.15 and 0.25 holes/unit cell, LSMO undergoes a simultaneous

magnetic and metal-insulator phase transition from a paramagnetic insulating state to a ferromagnetic metallic state upon cooling. Carrier-induced transitions between different phases of CMR materials have been achieved using electric currents, chemical doping, and band-gap engineering of p - n junction heterostructures.⁸⁻¹¹ These techniques involve structural modification, introduction of disorder, or manipulation of the band structure, which influence the magnetic properties in ways unrelated to the change in carrier concentration. For example, by modifying the mean radius $\langle r \rangle$ of the dopant using an isovalent cation, one can control the conduction bandwidth, thereby changing the transition temperature and the doping range of the FM phase.⁷

In this experiment, to provide the electric field that modulates the carrier concentration, we combine LSMO with a ferroelectric perovskite oxide, $\text{Pb}(\text{Zr}_x\text{Ti}_{1-x})\text{O}_3$ (PZT), in epitaxial thin film heterostructure form (Fig. 2). PZT can supply enormous spontaneous polarization fields, on the order of $15\text{--}45 \mu\text{C}/\text{cm}^2$, larger than the breakdown field of SiO_2 . In thin films, the voltages required to switch between polarization states are on the order of a few volts ($\sim 1 \text{ V}/1000 \text{ \AA}$). Recently, electrostatic approaches have been used to investigate a broad range of systems, such as dilute magnetic semiconductors and correlated complex oxides.¹²⁻²⁰

One challenge for the field effect approach in CMR materials is the nearly metallic hole-doping levels ($\sim 10^{21}$ holes/ cm^3) at which ferromagnetism occurs. At these charge densities, the length over which an applied electric field is screened is on the order of a few atomic spacings. As a result, ultrathin, atomically smooth CMR heterostructures are required to observe substantial modulation of the carrier density. Because PZT and LSMO both belong to the perovskite family of oxides and are thus structurally very similar, it is possible to realize such heterostructures in epitaxial, single-crystalline form.

To fabricate these structures, we used off-axis magnetron sputtering. For LSMO, we used a growth temperature of 660°C and a process gas consisting of $\sim 20\%$ O_2 and $\sim 80\%$ Ar at a pressure of 150 millitorr. The growth conditions for PZT are similar, but with a growth temperature of $\sim 500^\circ\text{C}$.²¹ We first examined the physical properties of

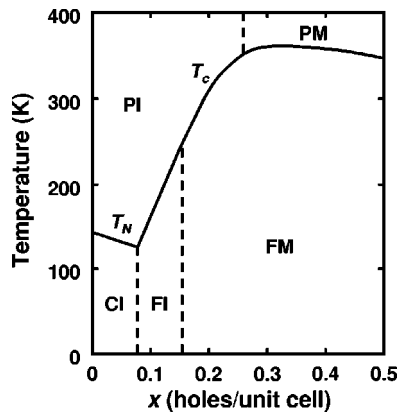


FIG. 1. Schematic temperature-doping phase diagram for the $\text{La}_{1-x}\text{Sr}_x\text{MnO}_3$ system, adapted from Ref. 7. PI denotes the paramagnetic insulator, CI the spin canted antiferromagnetic insulator, FI the ferromagnetic insulator, PM the paramagnetic metal, and FM the ferromagnetic metal.

single-layer LSMO films. Figure 3(a) shows a θ - 2θ diffraction scan taken on a 400 Å thick $\text{La}_{0.8}\text{Sr}_{0.2}\text{MnO}_3$ film deposited on single-crystal (100) SrTiO_3 , which reveals c -axis-oriented growth, with a lattice constant of ~ 3.85 Å. No other impurity phases are detected. The rocking curve taken around the 001 reflection has a typical full width at half maximum of 0.06° . Finite size oscillations around the 001 reflection, as shown in Fig. 3(b), are used to determine the film thickness and calibrate the deposition rate.

The surface quality of LSMO was investigated by atomic force microscopy (AFM). Figure 4 shows an AFM image of a 30 Å thick $\text{La}_{0.8}\text{Sr}_{0.2}\text{MnO}_3$ film. The film surface has a root-mean-square (rms) roughness of 1–2 Å and consists of atomically flat terraces a few thousand angstroms wide, separated by 2 Å atomic steps. These atomic steps are due to the slight miscut in the SrTiO_3 single-crystal substrate. PZT layers were deposited *in situ* on the LSMO films, which were patterned into four-point resistivity paths, and gold electrodes were deposited for electrical transport measurements.²² X-ray diffraction analyses reveal the growth of c -axis-oriented PZT, for which the polarization is normal to the surface (Fig. 5).²³ The rocking curve taken around the PZT 001 reflection has a full width at half maximum of

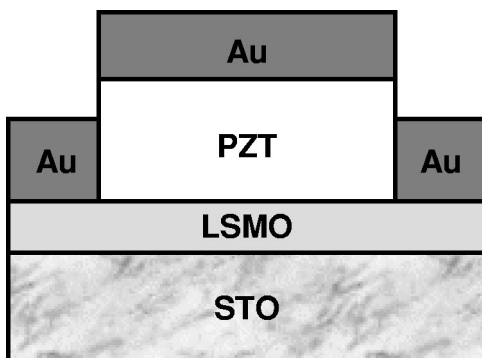


FIG. 2. Schematic view of a PZT/LSMO heterostructure deposited on a SrTiO_3 (STO) substrate. Gold electrodes are deposited for electrical transport measurements.

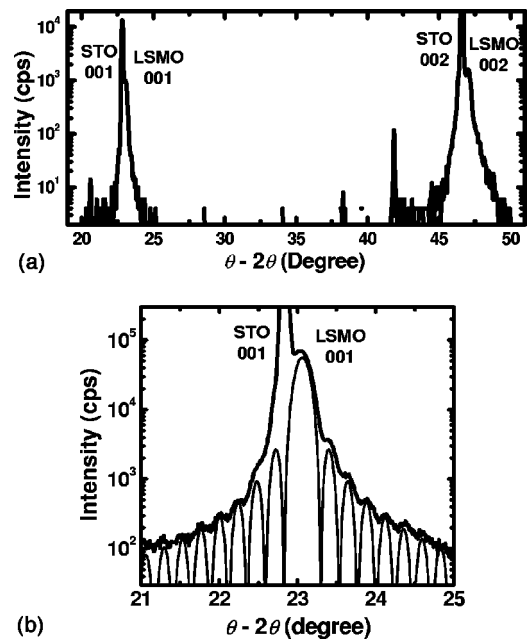


FIG. 3. (a) θ - 2θ x-ray diffraction scan taken on a 400 Å thick $\text{La}_{0.8}\text{Sr}_{0.2}\text{MnO}_3$ film; (b) high-resolution θ - 2θ scan, showing finite size oscillations around the 001 reflection (thick line), along with a calculated spectrum for a film with a thickness of 374 Å and a lattice constant of 3.85 Å (thin line).

$\sim 0.3^\circ$, and the typical rms roughness of the PZT/LSMO heterostructures is 4 Å.

We next examined the ferroelectric field effect modulation of the transport properties of the LSMO layer. In Fig. 6, we plot the resistivity as a function of temperature of a 3000 Å PZT/40 Å LSMO heterostructure, for the two polarization states of the ferroelectric. Switching between the two states is accomplished by applying a ± 5 V pulse across the PZT layer. The low resistivity curve corresponds to the polarization state that accumulates holes at the interface between the

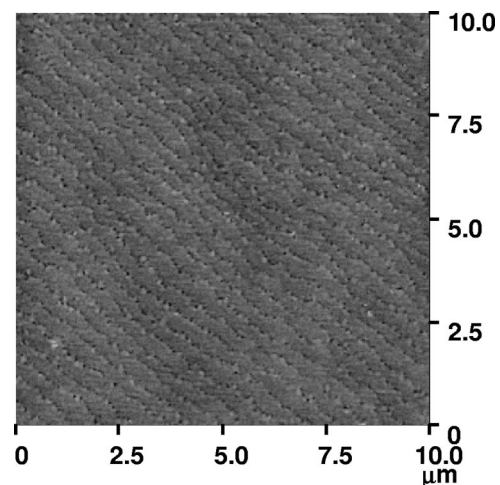


FIG. 4. Atomic force microscope image of the surface of a 30 Å LSMO film. The measured rms surface roughness is 1 to 2 Å. The image shows a series of terraces spaced a few thousand angstroms apart with a step height of 2 Å.

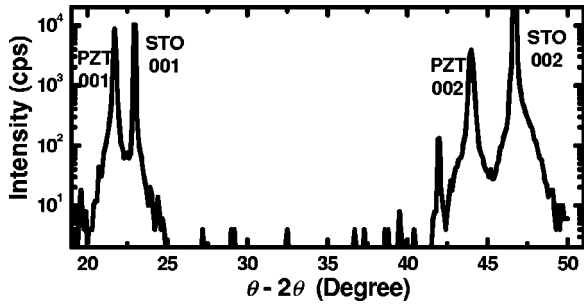


FIG. 5. $\theta-2\theta$ x-ray diffraction scan taken on a PZT/LSMO bilayer. The 001 reflection of the ultrathin LSMO layer cannot be resolved due to overlap with the substrate peak.

PZT and LSMO, thereby increasing the carrier concentration. The high resistivity curve corresponds to the opposite polarization state, which depletes the LSMO of holes. Switching between these resistivity states is reversible, and capacitance-voltage measurements exhibit an asymmetric butterfly shape due to the ferroelectric hysteresis.

At room temperature, the resistivity ratio of the two states (defined as ρ_{high}/ρ_{low}) is 1.28. It has been proposed that free polarons exist at temperatures well above T_C , which then condense into clusters upon cooling at a temperature scale $T^* > T_C$, resulting in coexisting insulating and metallic phases.^{24,25} In the polaronic state, the conductivity σ is given by³

$$\sigma(T) = \frac{\sigma_0 T_0}{T} \exp\left(-\frac{E_\sigma}{k_B T}\right), \tag{1}$$

$$\sigma_0 = \frac{x(1-x)e^2}{\hbar a}.$$

Here T_0 is the temperature equivalent of the optical phonon energy, E_σ is the activation energy for polaron hopping, and a is a constant on the order of the interatomic spacing. At fixed temperature, the conductivity is proportional to the product of the hole doping per unit cell x and the fractional

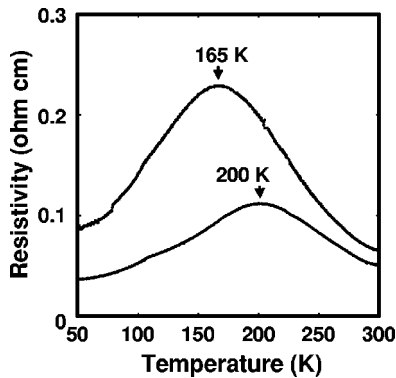


FIG. 6. Resistivity as a function of temperature for the two polarization states of the PZT layer. The upper curve corresponds to depletion of holes and is termed the depletion state; the lower curve corresponds to accumulation of holes and is termed the accumulation state. The resistivity peak temperatures are 165 K and 200 K for the depletion and accumulation states, respectively.

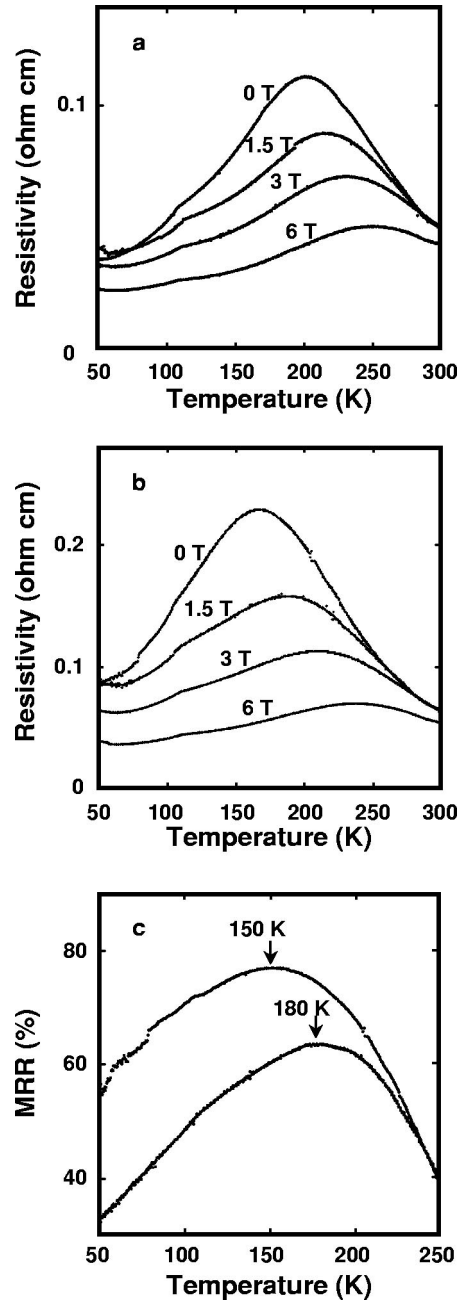


FIG. 7. Resistivity vs temperature for (a) the accumulation state and (b) the depletion state under applied magnetic fields of 0, 1.5, 3, and 6 T; (c) magnetoresistance ratio as a function of temperature at 6 T for both polarization states. The maximum magnetoresistance ratios are 64% for the accumulation state and 77% for the depletion state.

density of hopping sites $(1-x)$. While the applicability of this relation at room temperature requires detailed knowledge of T^* , we find within this picture that the measured resistivity change is consistent with the charge density modulation induced by a polarization of $\sim 30 \mu\text{C}/\text{cm}^2$.

As the temperature is lowered, we observe a transition from insulating to metallic behavior for both resistivity states, with the same temperature dependence that is observed in single-layer LSMO films in this doping range.²⁶

The peak temperatures in the resistivity curves, which coincide with the Curie temperatures, are 200 K for the accumulation state and 165 K for the depletion state.²⁷ The magnitude of the field effect is temperature dependent, but is roughly constant at temperatures well above T_C (>270 K). At 165 K, the resistivity ratio reaches 2.5.

Removing holes from the system decreases the Curie temperature by 35 K, a trend that agrees with the double exchange theory of magnetic ordering, which predicts that T_C is proportional to the carrier concentration.² Using this relationship, we find that a shift in T_C of 35 K corresponds to a carrier modulation of $\sim 20\%$, consistent with the magnitude of the ferroelectric polarization. In CMR systems, the Curie temperature is governed by the competition between the itinerancy of the electrons, which increases with carrier concentration and favors magnetic ordering, and the electron-phonon coupling, which localizes the electrons.^{28,29} This coupling is strongly affected by structural effects, such as distortions induced by chemical substitution. The field effect experiments here do not introduce such defect structures and show the relationship between changes in itinerancy and modulation of the transition temperature.

To further investigate the modulation of magnetism by the field effect, we studied the magnetotransport properties of these heterostructures. Figures 7(a) and 7(b) show the resistivity as a function of temperature for the two polarization states under magnetic fields of 0, 1.5, 3, and 6 T applied perpendicular to the film surface. The CMR effect is observed for both states, with the maximum magnetoresistance ratio (MRR) at 6 T occurring at ~ 180 K for the accumulation state and ~ 150 K for the depletion state. (The MRR is defined as $[R(0) - R(H)]/R(0)$.) The maximum MRR is 64% in accumulation, and increases to 77% in depletion [Fig. 7(c)]. The shift of the MRR peak temperature confirms the modulation of the Curie temperature by the field effect, and the relative magnitudes of the changes in T_C and MRR agree with the universal relation obtained from various manganites using the chemical doping approach.³⁰

The electrostatic modulation here reveals the independent role of the charge density in the CMR effect, an aspect that cannot be shown using chemical doping, where substitutional disorder and the charge density of the material are inextricably linked. In the phase separation scenario of CMR materials, Dagotto and co-workers and others have proposed that disorder leads to electronically phase-separated regions or clusters, with the electronic conduction occurring through percolation between the clusters.^{6,25} The transport between phase-separated regions is sensitive to magnetic fields and hence results in a colossal magnetoresistance effect. In this picture, the substitutional disorder plays a central role since it defines the sizes and density of the phase separated clusters and hence the magnitude of the CMR effect. In the electrostatic approach here, the level of disorder is untouched, and the modulation of T_C and magnetoresistance arises solely from changes in the charge density.

In conclusion, we have reversibly modulated the Curie temperature and magnetoresistance of a perovskite manganite using the polarization field of a ferroelectric, showing that modulating the carrier density of LSMO alone can lead to colossal effects. Applying this approach to other correlated systems can facilitate the study of charge-induced quantum phase transitions and can also be used to explore new magnetic materials. For example, one can seek metallic behavior in Mott insulators such as NiO, or ferromagnetic ordering in other correlated oxides. This approach can also lead to novel devices, such as magnetic switches based upon the local manipulation of magnetic behavior using electrostatic charge.¹⁴

We thank E. Dagotto, J. Reiner, S. Sachdev, J.-M. Triscone, J. Tully, and A. Vervekin for discussions and technical support. Low-temperature measurements were carried out on a Quantum Design Physical Property Measurement System. This research was sponsored by the Air Force Office of Scientific Research, the National Science Foundation, and the Packard Foundation.

¹C. Zener, Phys. Rev. **82**, 403 (1951).

²A. J. Millis, P. B. Littlewood, and B. I. Shraiman, Phys. Rev. Lett. **74**, 5144 (1995).

³M. B. Salamon and M. Jaime, Rev. Mod. Phys. **73**, 583 (2001).

⁴E. E. Narimanov and C. M. Varma, Phys. Rev. B **65**, 024429 (2001).

⁵L. Sheng, D. Y. Xing, D. N. Sheng, and C. S. Ting, Phys. Rev. B **56**, R7053 (1997).

⁶J. Burgy, M. Mayr, V. Martin-Mayor, A. Moreo, and E. Dagotto, Phys. Rev. Lett. **87**, 277202 (2001).

⁷M. Imada, A. Fujimori, and Y. Tokura, Rev. Mod. Phys. **70**, 1039 (1998).

⁸A. Asamitsu, Y. Tomioka, H. Kuwahara, and Y. Tokura, Nature (London) **388**, 50 (1997).

⁹Y. Tokura, A. Urushibara, Y. Moritomo, T. Arima, A. Asamitsu, G. Kido, and N. Furukawa, J. Phys. Soc. Jpn. **63**, 3931 (1994).

¹⁰M. Rajeswari, R. Shreekala, A. Goyal, S. E. Lofland, S. M.

Bhagat, K. Ghosh, R. P. Sharma, R. L. Greene, R. Ramesh, T. Venkatesan, and T. Boettcher, Appl. Phys. Lett. **73**, 2672 (1998).

¹¹H. Tanaka, J. Zhang, and T. Kawai, Phys. Rev. Lett. **88**, 027204 (2002).

¹²C. H. Ahn, J.-M. Triscone, N. Archibald, M. Decroux, R. H. Hammond, T. H. Geballe, O. Fischer, and M. R. Beasley, Science **269**, 373 (1995).

¹³S. Mathews, R. Ramesh, T. Venkatesan, and J. Benedetto, Science **276**, 238 (1997).

¹⁴C. H. Ahn, T. Tybell, L. Antognazza, K. Char, R. H. Hammond, M. R. Beasley, O. Fischer, and J.-M. Triscone, Science **276**, 1100 (1997).

¹⁵C. H. Ahn, S. Gariglio, P. Paruch, T. Tybell, L. Antognazza, and J.-M. Triscone, Science **284**, 1152 (1999).

¹⁶H. Ohno, D. Chiba, F. Matsukura, T. Omiya, E. Abe, T. Dietl, Y. Ohno, and K. Ohtani, Nature (London) **408**, 944 (2000).

¹⁷T. Wu, S. B. Ogale, J. E. Garrison, B. Nagaraj, A. Biswas, Z.

- Chen, R. L. Greene, R. Ramesh, T. Venkatesan, and A. J. Millis, *Phys. Rev. Lett.* **86**, 5998 (2001).
- ¹⁸J. H. Smet, R. A. Deutschmann, F. Ertl, W. Wegscheider, G. Abstreiter, and K. von Klitzing, *Nature (London)* **415**, 281 (2002).
- ¹⁹S. Gariglio, C. H. Ahn, D. Matthey, and J.-M. Triscone, *Phys. Rev. Lett.* **88**, 067002 (2002).
- ²⁰Y. D. Park, A. T. Hanbicki, S. C. Erwin, C. S. Hellberg, J. M. Sullivan, J. E. Mattson, T. F. Ambrose, A. Wilson, G. Spanos, and S. T. Jonker, *Science* **295**, 651 (2002).
- ²¹J.-M. Triscone, L. Frauchiger, M. Decroux, L. Mieville, O. Fischer, C. Beeli, P. Stadelmann, and G. A. Racine, *J. Appl. Phys.* **79**, 4298 (1996).
- ²²S. Gariglio, C. H. Ahn, and J.-M. Triscone, in *Proceedings of SPIE Volume 4058: Superconducting and Related Oxides: Physics and Nanoengineering IV*, edited by D. Pavuna and I. Bozovic (SPIE, Orlando, FL, 2000), p. 314.
- ²³For these experiments, we used $\text{Pb}(\text{Zr}_x\text{Ti}_{1-x})\text{O}_3$ with $x=0.2$.
- ²⁴G.-M. Zhao, K. Conder, H. Keller, and K. A. Müller, *Nature (London)* **381**, 676 (1996).
- ²⁵E. Dagotto, *Nanoscale Phase Separation and Colossal Magnetoresistance* (Springer, New York, 2003), Chaps. 16 and 19.
- ²⁶Below 50 K, the LSMO becomes insulating, which is observed in films with compositions near the FI-FM phase boundary [Y. Yamada, O. Hino, S. Nohdo, R. Kanao, T. Inami, and S. Katano, *Phys. Rev. Lett.* **77**, 904 (1996)].
- ²⁷A. Urushibara, Y. Moritomo, T. Arima, A. Asamitsu, G. Kido, and Y. Tokura, *Phys. Rev. B* **51**, 14 103 (1995).
- ²⁸A. J. Millis, R. Mueller, and B. I. Shraiman, *Phys. Rev. B* **54**, 5405 (1996).
- ²⁹H. Röder, J. Zang, and A. R. Bishop, *Phys. Rev. Lett.* **76**, 1356 (1996).
- ³⁰K. Khazeni, Y. X. Jia, L. Lu, V. H. Crespi, M. L. Cohen, and A. Zettl, *Phys. Rev. Lett.* **76**, 295 (1996).